Journal of Molecular Structure 1004 (2011) 193–203

Contents lists available at SciVerse ScienceDirect

Journal of Molecular Structure

journal homepage: www.elsevier.com/locate/molstruc

Experimental and theoretical anion binding studies on coumarin linked thiourea and urea molecules

Kumaresh Ghosh [a,*], Suman Adhikari [a], Roland Fröhlich [b], Ioannis D. Petsalakis [c], Giannoula Theodorakopoulos [c,*]

[a] Department of Chemistry, University of Kalyani, Kalyani, Nadia 741 235, India
[b] Organisch-Chemisches Institut, Universität Münster, Corrensstraβe 40, D-48149 Münster, Germany
[c] Theoretical and Physical Chemistry Institute, The National Hellenic Research Foundation, 48 Vassileos Constantinou Avenue, Athens 116 35, Greece

ARTICLE INFO

Article history:
Received 9 May 2011
Received in revised form 31 July 2011
Accepted 1 August 2011
Available online 23 August 2011

Keywords:
Coumarin-based urea and thiourea
Fluoride recognition
Benzoate recognition
Dicarboxylate recognition
Anion binding
DFT results

ABSTRACT

A series of coumarin linked thiourea and urea molecules **1**–**5** have been designed and synthesized. Thiourea-based monotopic receptors **1**–**4** showed selective sensing of F^- and $C_6H_5COO^-$ by exhibiting significant change in emission as well as change in color. The ditopic receptor **5**, on the other hand, fluorometrically distinguished isomeric aromatic dicarboxylates in polar solvent DMSO. Theoretical calculations have been carried out on systems **1**–**4** and their complexes with $C_6H_5COO^-$ and F^- anions in the presence of CH_3CN solvent. Calculations have been carried out to determine the geometry and bonding of the complexes in the ground electronic state as well as on the excited electronic states relevant to the absorption spectra and emission spectra in an effort to obtain information on the spectral changes accompanying complexation of the receptors **1**–**4** with the two anions.

1. Introduction

The development of simple molecular systems that can recognize and sense anions selectively through visible, electrochemical and optical responses has received considerable interest in recent years because of the important roles played by anions in biological, industrial and environmental processes [1]. Molecules with functional groups such as amides [2], ureas/thioureas [3], guanidinium [4] and ammonium [5] derivatives have proven to be particularly effective in this regard, as they are capable of binding anions using directional hydrogen bonding interactions. However, attachment of such functional groups with a suitable chromophoric part either covalently or intermolecularly provides a complete receptor module that can intimate binding information either by a color change, fluorescence or both. In an effort to develop fluorescent anion receptors, we previously reported coumarin-based chemosensors **1** and **2** for the selective recognition of anions [6] employing the criteria of PET sensing using the '*fluorophore–spacer–receptor*' model developed by de Silva for the detection of cations [1b]. Although several PET sensors for anions are known [7], no such thiourea-linked coumarin systems employing neutral anion receptors, was reported prior to our attempt that exhibit ideal PET behavior and color changes as signaling event, detectable by the naked eye, upon binding of anions. In this full account, we report here our extended approach to the synthesis of other coumarin-based receptors **3**–**5** of which **5** acts as ditopic receptor and their molecular recognition properties towards varieties of anions such as halides, HSO_4^-, $H_2PO_4^-$, as well as mono- and dicarboxylates in organic solvent. Theoretical calculations have been carried out on systems **1**–**4** and their complexes with $C_6H_5COO^-$ and F^- anions in the presence of CH_3CN solvent. Calculations to a smaller extent have been carried out on receptor **5** as well. The purpose of the calculations was (i) to determine the geometry and bonding of the complexes in the ground electronic state and (ii) to calculate the excited electronic states relevant to the absorption spectra and emission spectra in an effort to obtain information on the spectral changes accompanying complexation of the receptors **1**–**4** with the two anions.

2. Experimental section

Chemosensors **1** and **2** were easily synthesized [6] in good yields from readily available starting materials, following Scheme 1 in the Supplementary information. Chemosensors **3**–**5** were obtained in good yields, following Scheme 2. The 6-aminocoumarin

* Corresponding authors. Fax: +91 3325828282 (K. Ghosh).
E-mail addresses: ghosh_k2003@yahoo.co.in (K. Ghosh), idpet@eie.gr (I.D. Petsalakis), ithe@eie.gr (G. Theodorakopoulos).

0022-2860/$ - see front matter © 2011 Elsevier B.V. All rights reserved.
doi:10.1016/j.molstruc.2011.08.004

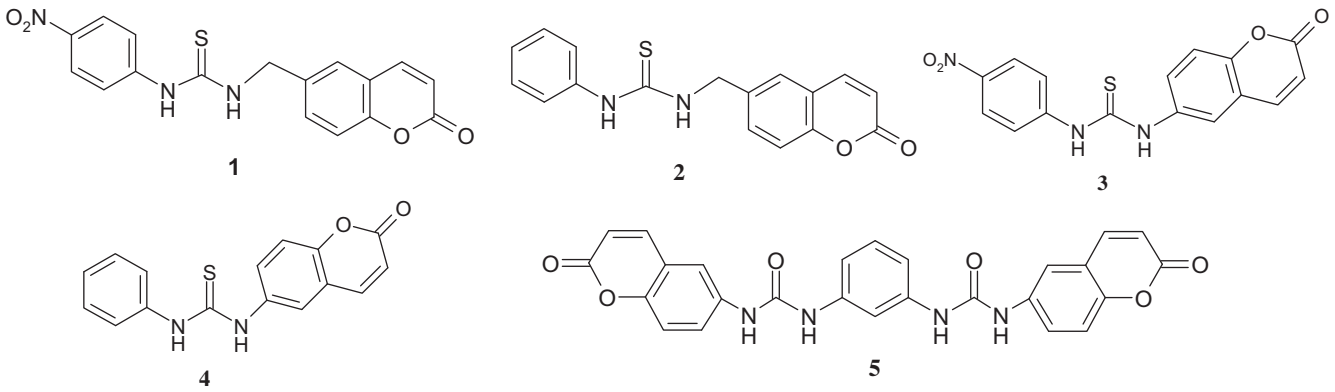

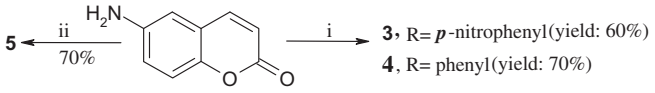

Scheme 2. Reagents and conditions: (i) RNCS in dry THF, (ii) phenyl-1,3-diisocyanate in dry THF.

was coupled with different isothiocyanates in dry THF under inert atmosphere at room temperature to afford **3** and **4** as pale yellow solids. Use of phenyl-1,3-diisocyanate in the coupling reaction gave the ditopic chemosensor **5**.

Structures of the receptors were established from the analysis of ^{1}H NMR, ^{13}C, mass, FT-IR spectral data and also by solving single crystal X-ray structures in case of **2** and **4**.

2.1. 1-(4-Nitrophenyl)-3-((2-oxo-2H-chromen-6-yl))thiourea (3)

To a stirred solution of 6-aminocoumarin (0.1 g, 0.62 mmol) in dry THF (15 mL) containing few drops of dry DMF, was added *p*-nitrophenyl isothiocyanate (0.123 g, 0.68 mmol) at room temperature. The reaction mixture was stirred overnight at room temperature. After completion of reaction, the solvent was evaporated and the residue was purified by column chromatography using 4% CH_3OH in $CHCl_3$ as eluent to give **3** as yellowish powder, (0.127 g, yield: 60%); mp 197–199 °C; ^{1}H NMR (400 MHz, d_6-DMSO): δ 9.69 (s, 1H, urea NH), 9.45 (s, 1H, urea NH), 8.11 (d, 2H, J = 8 Hz), 7.90 (d, 2H, J = 8 Hz), 7.78 (s, 1H), 7.64 (1 d, H, J = 8 Hz), 7.46 (d, 1H, J = 8 Hz), 7.23 (d, 1H, J = 8 Hz) 6.33 (d, 1H, J = 8 Hz), ^{13}C NMR (125 MHz, d_6-DMSO): δ 179.7, 159.7, 150.6, 145.9, 143.9, 142.3, 135.1, 128.3, 124.2, 123.2, 121.6, 118.5, 116.3, 112.2, FT-IR: ν cm^{-1} (KBr): 3275, 2923, 1720, 1635, 1464, 1174, Mass (EI): 342.2 $[M + H]^+$, 311.1, 260.5, 247.1, $C_{16}H_{13}N_3O_4S$: calcd. C 55.97, H 3.82, N 12.24; found C 55.90, H 3.74, N 12.17.

2.2. 1-((2-Oxo-2H-chromen-6-yl)-3-phenylthiourea (4)

To a stirred solution of 6-aminocoumarin (0.100 g, 0.57 mmol) in dry THF (15 mL) was added phenyl isothiocyanate (0.08 mL, 0.66 mmol) at room temperature. The reaction mixture was stirred overnight at room temperature. After completion of reaction, the solvent was evaporated and the residue was chromatographed using 50% ethyl acetate in benzene as eluent to give **4** as white crystalline product (0.110 g, yield: 70%); mp 158–160 °C; ^{1}H NMR (400 MHz, d_6-DMSO): δ 9.94 (s, 2H, urea NH), 8.08 (d, 1H, J = 8 Hz), 7.81 (br s, 1H), 7.64 (d, 1H, J = 8 Hz), 7.47 (d, 2H, J = 8 Hz), 7.39–7.32 (m, 3H), 7.15 (t, 1H, J = 8 Hz), 6.50 (d, 1H, J = 8 Hz), ^{13}C NMR (125 MHz, d_6-DMSO): δ 180.3, 160.4, 151.2, 143.2, 137.6, 135.0, 129.0, 128.6, 126.0, 124.5, 123.5, 118.5, 116.7, 116.6, FT-IR: ν cm^{-1} (KBr): 3269, 1714, 1622, 1572, 1538, 1494, 1290, Mass (EI): 297.2 $[M + H]^+$, 288.2, 263.1, $C_{16}H_{14}N_2O_2S$: calcd. C 64.41, H 4.73, N 9.39; found C 64.32, H 4.69, N 9.33.

2.3. 1,1′-(1,3-Phenylene)bis(3-(2-oxo-2H-chromen-6-yl)urea (5)

To a stirred solution of 6-aminocoumarin (0.150 g, 0.93 mmol) in dry THF (20 mL) was added phenyl 1, 3 diisocyanate (0.074 g, 0.46 mmol) at room temperature. The reaction mixture was stirred for 24 h at room temperature. After completion of reaction, the solvent was removed under vacuo, the crude product obtained was recrystallised from $CHCl_3$ to give **5** as white solid (0.314 g, yield: 70%); mp > 300 °C; ^{1}H NMR (400 MHz, d_6-DMSO): δ 8.82 (s, 2H, urea NH), 8.78 (s, 2H, urea NH), 8.07 (d, 2H, J = 8 Hz), 7.90 (d, 2H, J = 6.8 Hz), 7.74 (s, 1H), 7.57 (dd, 2H, J_1 = 8 Hz, J_2 = 2.4 Hz), 7.35 (d, 2H, J = 8 Hz), 7.18 (t, 1H, J = 8 Hz), 7.07 (d, 2H, J = 8 Hz), 6.48 (d, 2H, J = 8 Hz), ^{13}C NMR (125 MHz, d_6-DMSO): δ 160.1, 152.4, 148.6, 144.3, 139.9, 136.1, 129.0, 122.5, 118.7, 116.6, 116.5, 116.4, 111.8. 108.0, FT-IR: ν cm^{-1} (KBr): 3383, 1715, 1691, 1679, 1544, 1438, 1185, Mass (EI): 505.0 $[M + Na]^+$, $[M + H]^+$ 483.3, 353.8, $C_{26}H_{22}N_4O_6$: calcd. C 64.19, H 4.56, N 11.52; found C 64.10, H 4.49, N 11.48.

3. Results and discussion

The anion binding properties of thiourea-based monotopic receptors **1**–**4** were investigated by observing the changes in their emission, absorption spectra in CH_3CN and ^{1}H NMR in $CDCl_3$.

3.1. UV–vis, fluorescence and crystallographic studies

In the earlier report [6] we demonstrated the anion recognition properties of **1** and **2** in CH_3CN (containing 0.08% DMSO for homogeneity of the solution). UV titration of **1** ($c = 5.63 \times 10^{-5}$ M), which exhibited a broad strong absorption band at 330 nm due to the coumarin moiety, was carried out with anions such as tetrabutylammonium fluoride, bromide, iodide, hydrogen sulfate, dihydrogen phosphate and benzoate. Upon addition of fluoride (F^-), the intensity of the absorption peak at 330 nm was remarkably reduced with simultaneous growth of a new peak at 455 nm and the almost colorless solution turned yellow brown [6]. The change in absorbance of **1** at 330 nm with the concentration of F^- was almost linear [6]. In the case of benzoate, the absorption peak at 330 nm shifted to 348 nm ($\Delta\lambda$ = 18 nm) with a concomitant decrease in intensity of the absorption and the solution turned light green in color [6]. The change in absorbance of **1** at 330 nm with the concentration of benzoate was also almost linear as that of **1** with F^-. The presence of isosbestic points during titration with both F^- and $C_6H_5COO^-$ revealed the formation of 1:1 complexes. No significant change in absorption

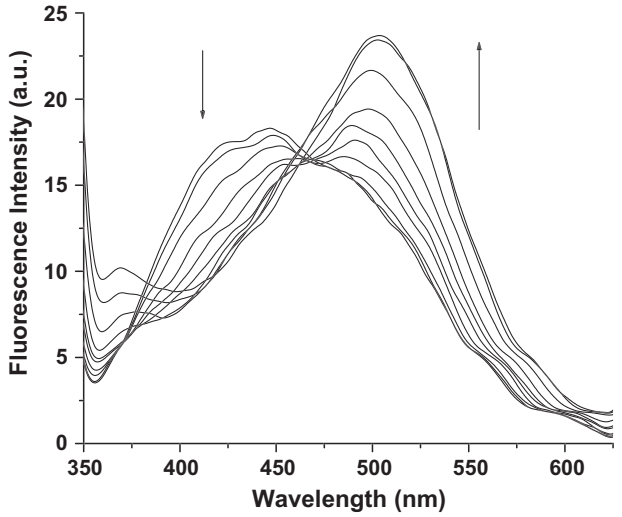

Fig. 1. Change in fluorescence spectra for **3** ($c = 5.86 \times 10^{-5}$ M) in CH_3CN upon addition of tetrabutylammonium fluoride.

Fig. 3. Color changes observed: (a) receptor **3**, (b) on addition of benzoate and (c) on addition of fluoride.

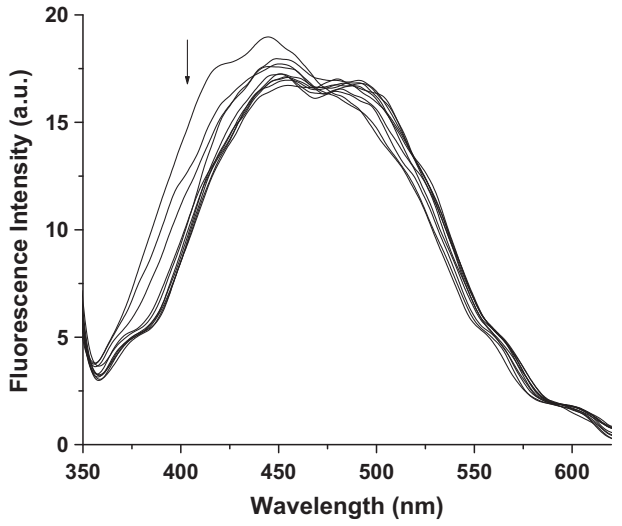

Fig. 2. Change in fluorescence spectra for **3** ($c = 5.86 \times 10^{-5}$ M) in CH_3CN upon addition of tetrabutylammonium benzoate.

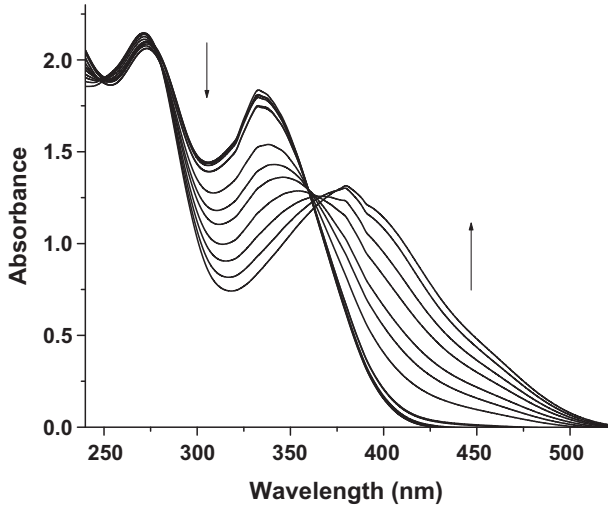

Fig. 4. Change in UV–vis spectra for **3** ($c = 5.86 \times 10^{-5}$ M) in CH_3CN upon addition of tetrabutylammonium fluoride.

or a noticeable color change was observed for **1** with other anions such as Br^-, I^-, $H_2PO_4^-$ and HSO_4^-.

The fluorescence emission spectra of **1** ($c = 4.51 \times 10^{-4}$ M) showed a broad band at 420 nm when excited at 380 nm (red edge excitation). With the addition of anions such as $C_6H_5COO^-$ and F^- as tetrabutylammonium salts, the emissions were ca. 88% and 99.6% '*switched off* 'or quenched, due to the formation of anion-receptor hydrogen bonded complexes [6]. During the titration there were no other observable changes in the emission spectra Addition of $H_2PO_4^-$ and HSO_4^-, hardly affected the emission spectra suggesting their weak interactions with the receptor site. The spherical ions such as Br^- and I^- did not cause any significant quenching of emission (see Stern–Volmer plot in Supporting information), thereby ruling out quenching by the heavy atom effect. Addition of F^-, $C_6H_5COO^-$, Br^-, I^-, $H_2PO_4^-$ and HSO_4^- as tetrabutylammonium salts to a solution of **2** in CH_3CN (containing 0.08% DMSO) resulted in a minor change in the UV–vis spectrum of receptor **2** and did not result in any new peaks at higher wavelengths or color changes of the solution. The fluorescence changes of **2** upon addition of F^- and $C_6H_5COO^-$ were significant but smaller compared to **1**. The fluorescence emissions at 369 nm ($\lambda_{ex} = 320$ nm) were ca. 12 and 19% '*switched off*' for $C_6H_5COO^-$ and F^-, respectively [6]. The smaller degree of quenching of emission in **2** was ascribed to a weak hydrogen bonding interaction between the less acidic thiourea protons and anions. This is reflected in their binding constant values (Ka: for **1**.F^- $5.78 \times 10^3\ M^{-1}$, for **2**.F^- $2.26 \times 10^3\ M^{-1}$, for **1**.$C_6H_5CO_2^-$ $2.02 \times 10^4\ M^{-1}$ and for **2**.$C_6H_5CO_2^-$ $1.04 \times 10^4\ M^{-1}$), which were measured by following the change in absorbance as a function of the concentration of the anions [8]. The association constants for both the receptors with benzoate are greater than F^-. This is purely due to strong hydrogen bonding interactions instead of deprotonation as observed in the case of fluoride, established by ^1H NMR [6].

In the present work we examined the binding interactions of **3** and **4** towards the same anions as considered for **1** and **2**. In both **3** and **4**, thiourea-binding sites are directly attached to the fluorescent probe. Interestingly, these two coumarin-based thiourea receptors behaved differently from **1** and **2** with respect to the selectivity and sensitivity toward anions. Receptor **3** exhibited the emission at 434 nm when excited at 330 nm in CH_3CN. Upon addition of the

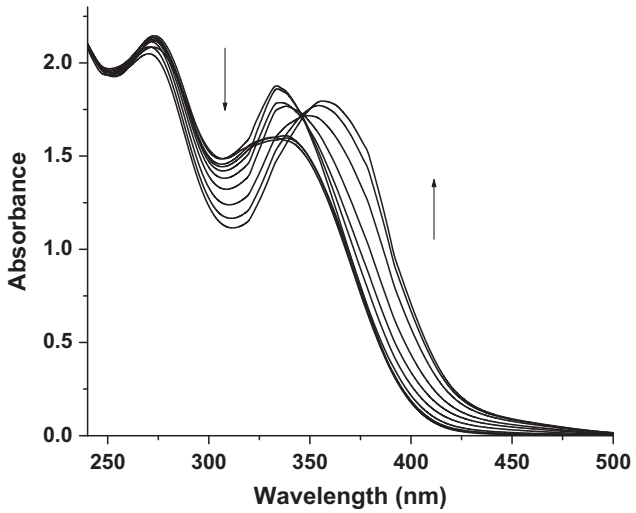

Fig. 5. Change in UV–vis spectra for **3** ($c = 5.86 \times 10^{-5}$ M) in CH_3CN upon addition of tetrabutylammonium benzoate.

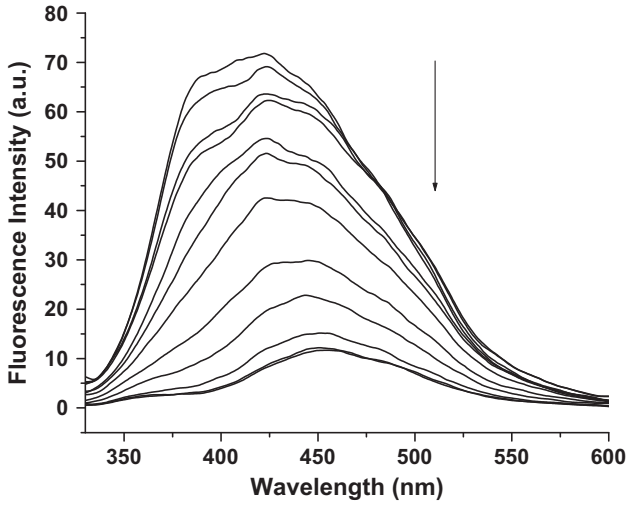

Fig. 7. Change in fluorescence spectra for **4** ($c = 5.4 \times 10^{-5}$ M) in CH_3CN upon addition of tetrabutylammonium fluoride.

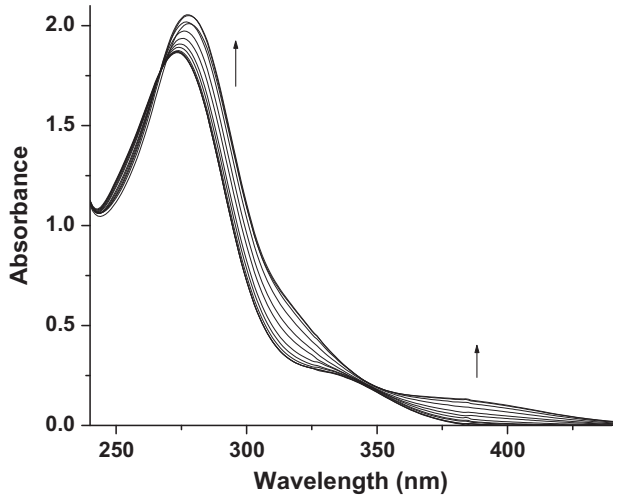

Fig. 6. Change in UV–vis spectra for **4** ($c = 5.4 \times 10^{-5}$ M) in CH_3CN upon addition of tetrabutylammonium fluoride.

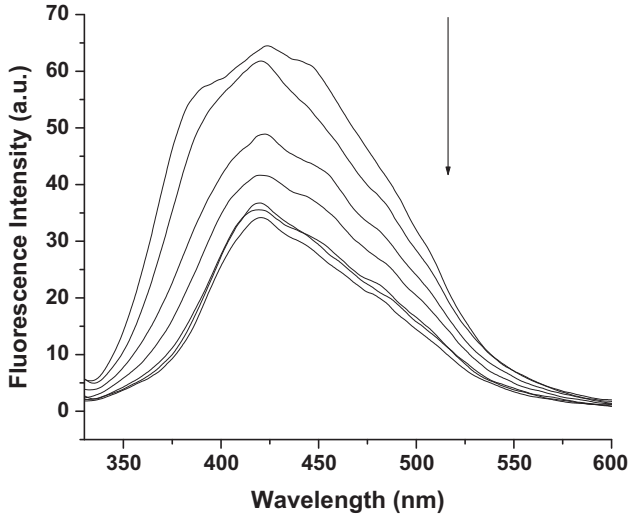

Fig. 8. Change in fluorescence spectra for **4** ($c = 5.4 \times 10^{-5}$ M) in CH_3CN upon addition of tetrabutylammonium benzoate.

anions the emission of **3** was perturbed to the different extents. Except for F^- and $C_6H_5COO^-$ ions, the emission of **3** was changed negligibly. Figs. 1 and 2 display the change in emission of **3** in the presence of F^- and $C_6H_5COO^-$, respectively. In the presence of increasing concentrations of F^-, the intensity of emission centered at 437 nm as a broad doublet decreased gradually with simultaneous growth of a new peak at 503 nm accompanying an isosbestic point at 464 nm (Fig. 1). During the course of titration, the color of the solution of **3** was changed from colorless to light red in the presence of F^- (Fig. 3). As shown in Fig. 4, the solution of **3** ($c = 5.86 \times 10^{-5}$ M) has the original absorption peak at 335 nm, which is due to the coumarin moiety. The absorption peak at 335 nm decreases, whereas the absorption peak at 380 nm increases by F^- titration, accompanying the formation of an isosbestic point at 364 nm. This signified the 1:1 binding interaction. As the corresponding result of visual inspection, the addition of $C_6H_5COO^-$ led to similar spectral change but the change was small (Fig. 5). However, as the $H_2PO_4^-$, Br^-, HSO_4^- and I^- were titrated into **3**, the spectra hardly changed even when the anions were in excess.

Given the fact that F^- is a strong Lewis base and can deprotonate one or more of the N–H protons of the receptor (as demonstrated by Gale and coworkers [9], Fabbrizzi et al. and others [10]), one would have expected that such a deprotonation should occur with the addition of the 2 equiv of F^- to **3**. However, this does not seem to be the case and only upon addition of a large excess of F^- this deprotonation occurs. Such deprotonation would give rise to the formation of HF_2^- [11] with concomitant changes in the absorption spectra, which would be shifted to longer wavelengths [12]. Indeed this was found to be the case for **3** at high F^- concentrations. Hence, we can conclude that for F^-, the binding occurs only through hydrogen bonding within a certain concentration range and deprotonation occurs when it remains in excess in solution (established by ^1H NMR study also; see latter).

Receptor **4** interacted with the anions weakly due to less acidic character of thiourea protons in **4** compared to **3**. In both fluorescence and UV, the spectral changes of **4** were observed in CH_3CN only in the presence of F^-. For other anions the changes were minor. Fig. 6 represents the change in absorption spectra of **4** in CH_3CN upon increasing addition of F^-. Figs. 7 and 8 demonstrate the change in emission of **4** in CH_3CN during titration with F^- and $C_6H_5COO^-$, respectively. The binding selectivity of **3** and **4** was evaluated in

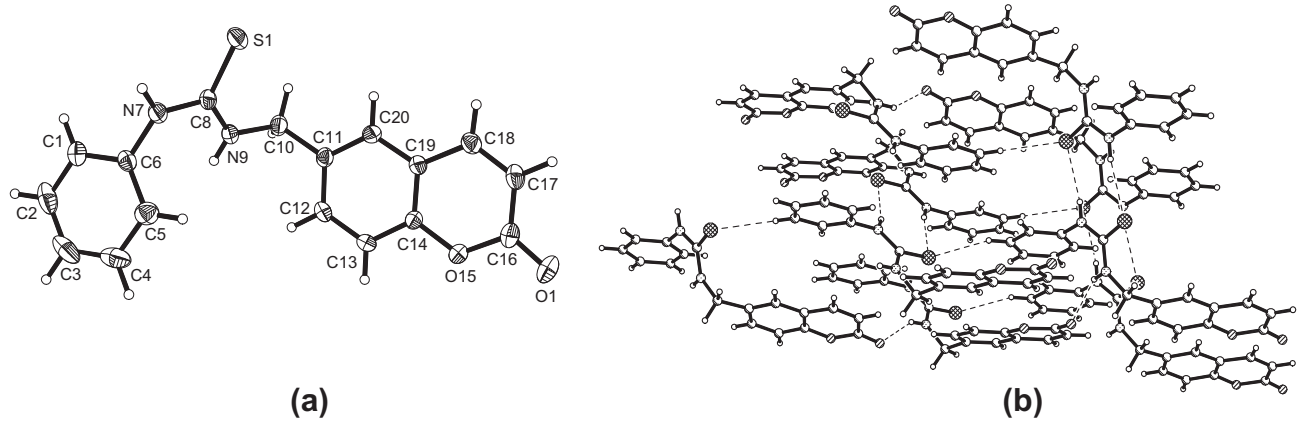

Fig. 9. (a) XP plot with atom numbering scheme and (b) packing view of **2**.

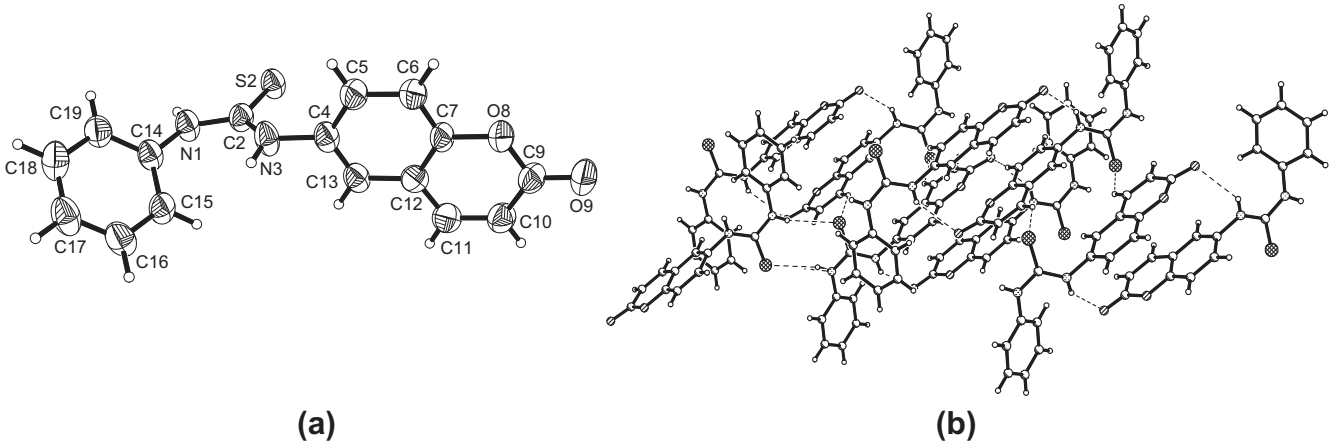

Fig. 10. (a) XP plot with atom numbering scheme and (b) packing view of **4**.

the ground state by determining the association constant values using the UV titration data [8] and we were able only to determine with F^- (K_a: for **3**.F^- 4.51×10^3 M^{-1}, for **2**.F^- 1.22×10^3 M^{-1}).

Guest induced quenching of emission of all the receptors is attributed to the activation of PET process occurring in between the binding site and fluorophore probe. The non-covalent interactions altogether enhance the efficiency of the PET process. The high degree of fluorescence quenching is believed to result from the increase in the reduction potential of the thiourea receptor moieties after anion recognition. This increases the rate of electron transfer from the HOMO of the thiourea-anion complex to the coumarin-excited state and encourages the PET process. It appears that the deprotonated species LH^-/L^{2-}, being more electron rich compared to the hydrogen-bonded complex with benzoate, activates the PET process more efficiently and shows greater quenching. Thus among the monotopic receptors **1**–**4**, receptors **1**, **2** which are different from **3** and **4** due to the presence of the $-CH_2$-group in between the binding site and the coumarin probe, are promising. The presence of the $-CH_2$-group controls the orientation of the thiourea binding site around the coumarin for which **1** and **2** behave differently from **3** and **4** in emission. To get an insight into this we solved the single crystal structures of **2** and **4** although the behavior of the molecules in solution is expected to be different. In the solid state it is found that compound **2** follows a different packing structure from **4**. The thiourea functional group in both structures is involved in intermolecular hydrogen bonding through the *anti* form and assembles the molecules in such a way that the disposition of the coumarin moiety varies. Figs. 9 and 10 represent the packing views of compounds **2** and **4**, respectively along with their XP plots. (Thermal ellipsoids are shown on the 50% probability level.) Crystal data are shown in the Supporting information.

The *anti* form of the thiourea group in some cases is found to be dominated over the *syn* form (*cf.* urea) [13] and accordingly, the possibility of the *anti* form of the thiourea in the binding of anions in solution cannot be ruled out. However, the maximum number of hydrogen bond formation of the thiourea receptors via *syn* form with the anions in solution is possibly a reason for their conformational preference over the *anti* form. This is quite understandable from the complexation induced downfield shifting of the thiourea protons in ^1H NMR (Supporting information). The situation is meaningless when the anions are present with the receptors in the solution in excess. In this circumstance, the most acidic thiourea proton is deprotonated and the preference of the *syn* or *anti* form of the thiourea moiety in binding of anions becomes irrelevant.

During interaction the color change in the host solutions of **1** and **3** is ascribed to the charge-transfer interactions between the electron-rich thiourea–anion complex donor unit and the electron-deficient *p*-nitrophenyl moiety [14].

3.2. ^1H NMR study

To understand the binding events further, ^1H NMR experiments were carried out in $CDCl_3$ like that of **1** and **2** [6]. In the present case, the large downfield chemical shift of the thiourea protons of **3** in the presence of F^- and $C_6H_5COO^-$ also indicated the strong

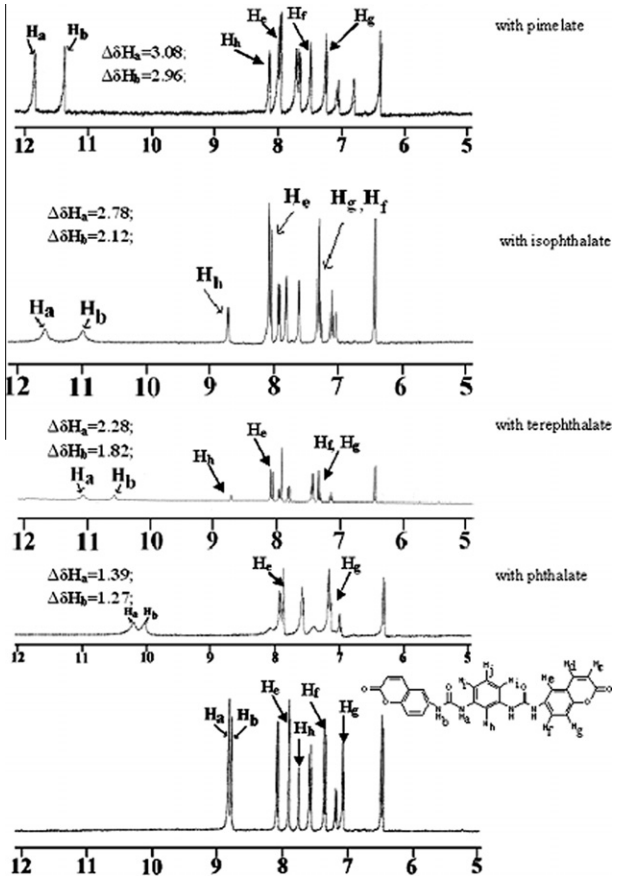

Fig. 11. Partial ^{1}H NMR (400 MHz) of **5** in DMSO-d_6 and its 1:1 complexes with different dicarboxylates.

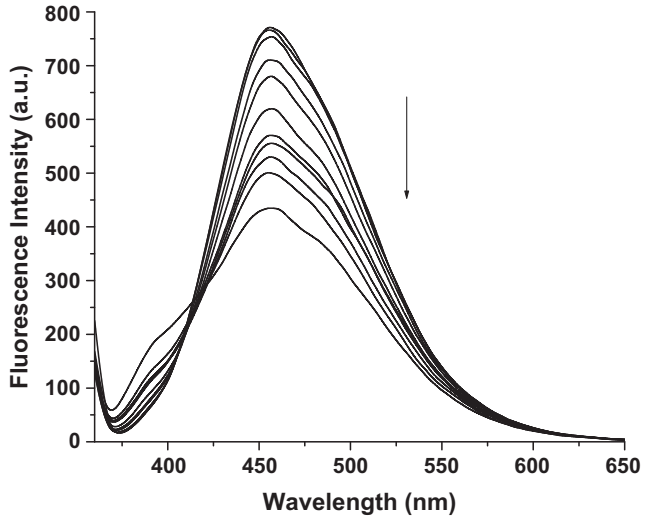

Fig. 12. Change in fluorescence spectra for **5** ($c = 4.15 \times 10^{-5}$ M) in DMSO upon addition of tetrabutylammonium isophthalate.

hydrogen bonded interaction (Supporting information). Upon complexation of F^-, the thiourea protons of **4** were also deprotonated in $CDCl_3$ like the cases of **1** and **3** with F^-.

Since urea/thiourea functionalities bind carboxylate anion involving directed hydrogen bonds, we intended to extend the scope of dicarboxylate ion recognition employing our designed and synthesized ditopic coumarin-receptor **5**.

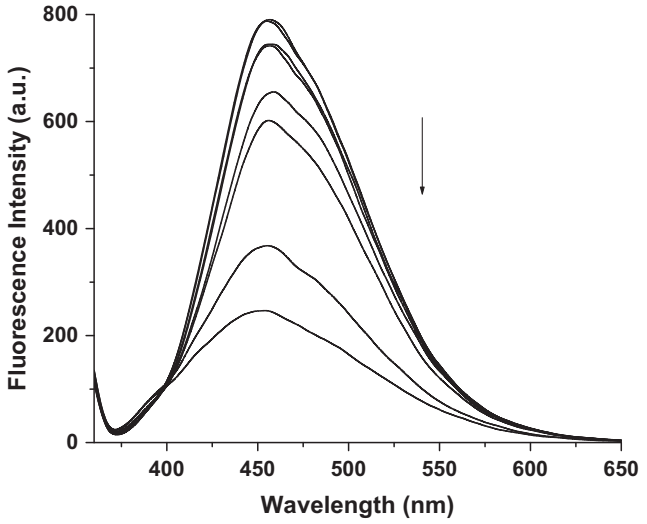

Fig. 13. Change in fluorescence spectra for **5** ($c = 4.15 \times 10^{-5}$ M) in DMSO upon addition of tetrabutylammonium pimelate.

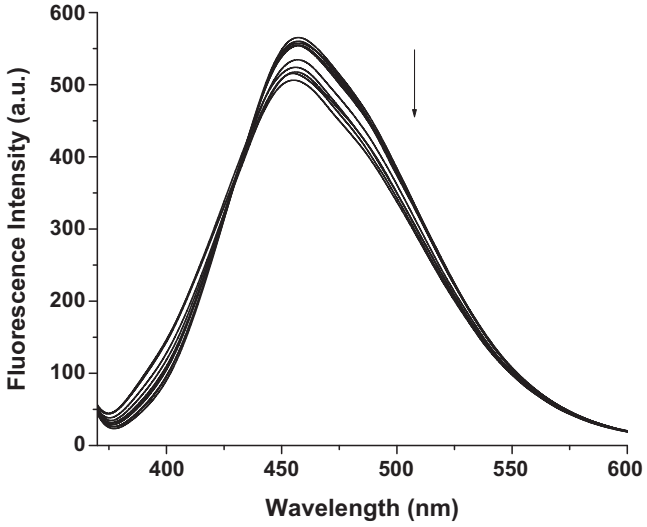

Fig. 14. Change in fluorescence spectra for **5** ($c = 4.15 \times 10^{-5}$ M) in DMSO upon addition of tetrabutylammonium succinate.

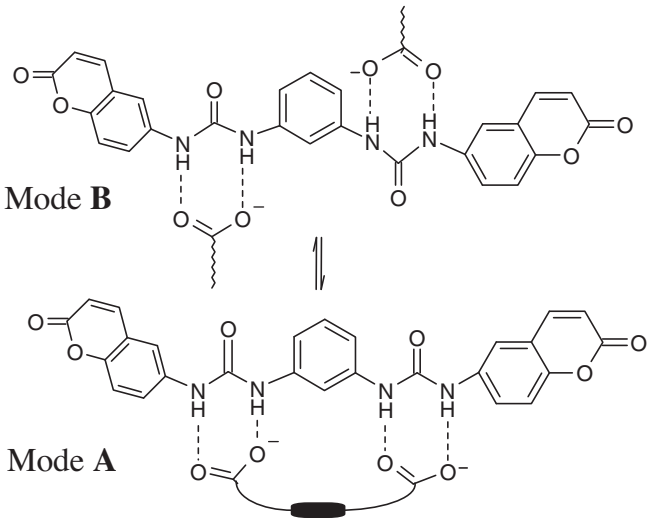

Fig. 15. Possible modes of complexation of dicarboxylates with **5**.

Table 1
Association constants of receptor **5** with anions in DMSO determined by UV method.

Guest anions[a]	Receptor **5** (K_a in M^{-1})[c]
$C_6H_5COO^-$	–[b]
Isophthalate	2.51×10^3
Pimelate	2.605×10^3
AcO-	–[b]
Terephthalate	8.21×10^2
Phthalate	–[b]
Succinate	–[b]

[a] Anions were used as their tetrabutylammonium salts.
[b] The changes were too small to calculate precisely.
[c] Errors in K_a were ⩽10%.

Table 2
Association constants of receptor **5** with anions in DMSO determined by fluorescence method.

Guest anions[a]	Receptor **5** (K_a in M^{-1})[c]
$C_6H_5COO^-$	–[b]
Isophthalate	5.27×10^3
Pimelate	4.33×10^3
AcO-	–[b]
Terephthalate	8.11×10^2
Phthalate	7.55×10^2
Succinate	–[b]

[a] Anions were used as their tetrabutylammonium salts.
[b] The changes were too small to calculate precisely.
[c] Errors in K_a were ⩽10%.

3.3. Complexation studies on ditopic receptor 5

Prior to the UV–vis and fluorescence studies, we recorded ^1H NMR of **5** in the absence and presence of the different dicarboxylates. Fig. 11 represents the spectral changes of **5** in the presence of equivalent amount of different dicarboxylates in d_6-DMSO. It is evident from Fig. 11 that the urea protons in **5** moved downfield upon complexation. In addition, the isophthaloyl peri proton (H_h) and the coumarin ring proton (H_e) also underwent downfield shift during interaction. Such downfield shifting of the interacting protons was indicative of short hydrogen bonding between the urea motif of **5** and the dicarboxylates.

The effect on the absorption and emission spectra of the urea-based molecule **5** was recorded in the presence of anions, using tetrabutylammonium salts in DMSO. The absorbance spectrum of **5** in presence of increasing concentrations of the guest anions (in DMSO) such as different dicarboxylates, was not greatly affected. This indicated poor interaction of **5** with the anions in the ground state. Only in presence of tetrabutylammonium salts of pimelic and isophthalic acids, the absorbance at 353 nm was changed accompanying isosbestic points at 371 and 374 nm, respectively (Supporting information). In comparison, the dicarboxylates such as phthalate, and terephthalate, which are isomeric to isophthalate did not change the absorbance of **5** significantly.

In the absence of anions, **5** ($c = 4.2 \times 10^{-5}$ M) showed a characteristic emission band at 455 nm when excited at 350 nm. Upon successive addition of guests, the intensity of the emission band gradually decreased to different extents for various dicarboxylates without producing any significant spectral change (i.e. no spectral shift or formation of new emission band). The degree of quenching in emission varied with the nature of the dicarboxylates as evident from the Stern–Volmer plot (Fig. S3).

Among the different dicarboxylates studied, only isophthalate and pimelate brought marked change in emission spectra. Figs. 12 and 13 represent the change in emission of **5** upon gradual addition of isophthalate and pimelate, respectively. The insignificant change of emission of **5** upon titration with succinate is displayed in Fig. 14. The stoichiometry of the complexes was confirmed from the break of the titration curves at [G]/[H] = 1 (Supporting information). The stoichiometry of complexes was additionally confirmed by Job's plots. Surprisingly, receptor **5** achieved 1:1 complexation with all the dicarboxylates studied in the present case irrespective of their nature. This is presumed to be due to the flexible nature of the *m*-xylene spacer in **5**, for which the dimensionally fitted dicarboxylates are involved in the formation of discrete 1:1 complexes in the mode **A** and overlong dicarboxylates induce dynamic 1:1 supramolecular structures *via* the mode **B** (Fig. 15). Both forms **A** and **B** remain equilibrium in solution. Reversibility of the complexation was confirmed by the addition of methanol into the DMSO solutions of receptor **5**-isophthalate and receptor **5**-pimelate. To realize the binding potencies of **5** with the anions we used both emission and absorption data for the determination of binding constant values [8]. As can be seen from Tables 1 and 2, the open cleft of **5** shows moderate affinities for isophthalate and pimelate. Other dicarboxylates such as phthalate and terephthalate, which are isomeric to isophthalate interacted weakly and showed lower binding constant values. The binding constant values determined by UV and fluorescence methods are of similar trend.

4. Details of the calculations

Geometry optimizations for the receptors **1–4** and the corresponding complexes with benzoate anion and with fluoride anion

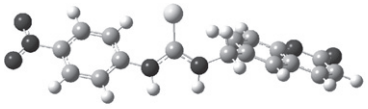

Receptor **1**: N-H (a) 1.01279 Å, N-H (b) 1.01306 Å

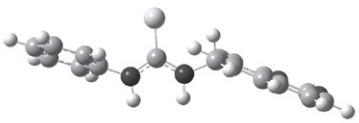

Receptor **2** : N-H (a) 1.01312 Å, N-H (b) 1.01244 Å

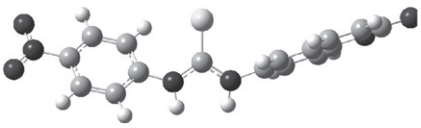

Receptor **3**: N-H (a) 1.01323 Å, N-H (b) 1.01321 Å.

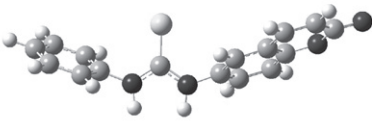

Receptor **4** : N-H (a) 1.01311 Å, N-H (b) 1.01291 Å.

Fig. 16. Optimized geometries of the receptors showing the amide N–H bond lengths.

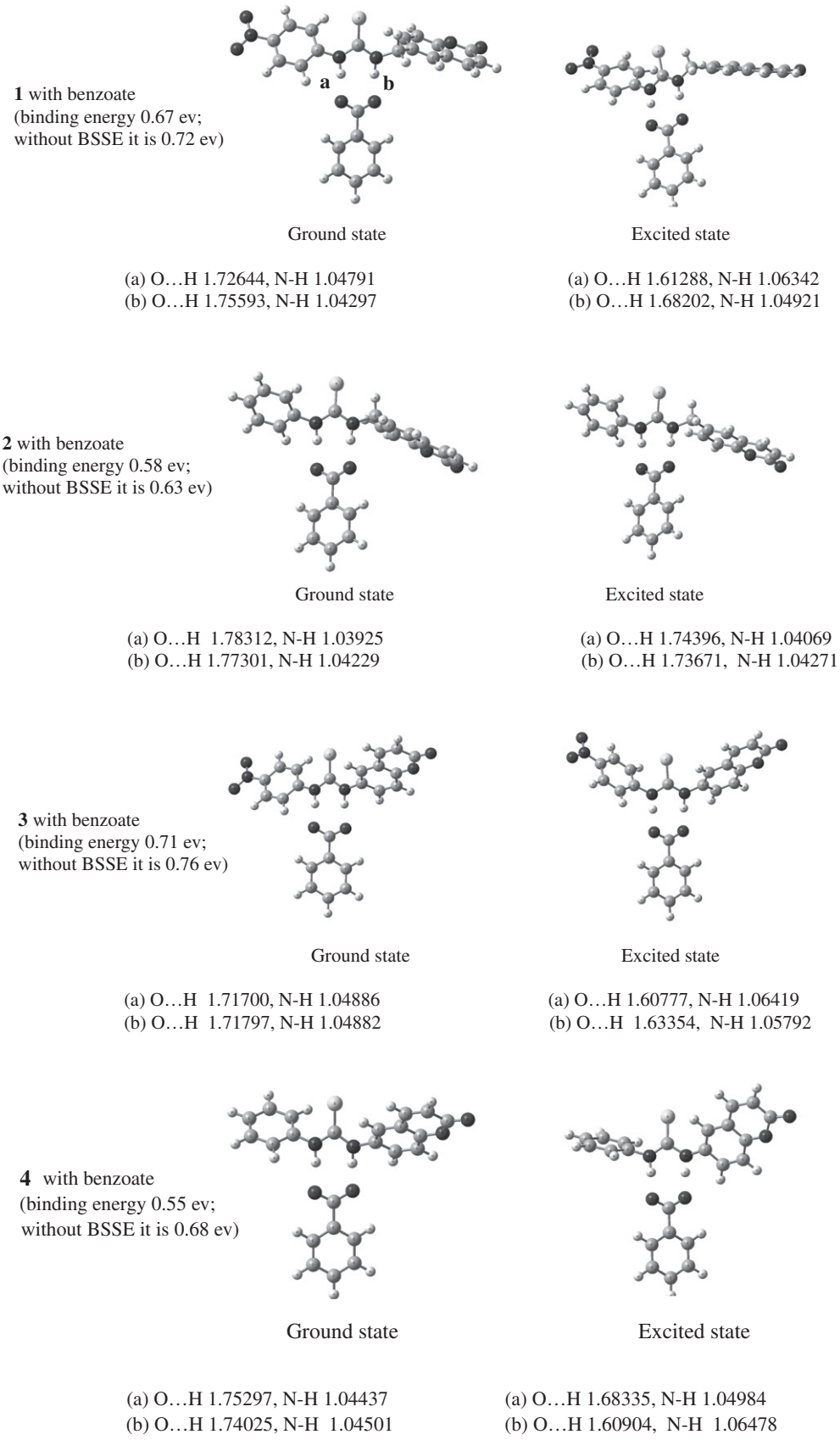

Fig. 17. Optimum geometries of ground and the first excited electronic states of the complexes of receptors with benzoate.

have been carried out by density functional theory (DFT) [15] calculations employing the CAM-B3LYP functional [16] and the 6-31+G(d, p) basis set. At the optimum geometries, time dependent density functional theory (TDDFT) [17] calculations were carried

Table 3
Absorption and emission maxima λ and oscillator strengths (f) of the three low-energy strongest transitions in receptors **1**–**4** and the complexes formed with F^- and with benzoate anion, obtained by TDDFT/CAM-B3LYP calculations.

Complex	Absorption			Emission		
	λ (nm), f	λ (nm), f	λ (nm), f	λ (nm), f	λ (nm), f	λ (nm), f
(**1**)	331, 0.638	322, 0.114	295, 0.484	485, 0.104	365, 0.017	315, 0.509
(**1**)+benzoate	361, 0.819	330, 0.029	299, 0.521	504, 0.170	377, 0.132	334, 0.539
(**1**)+F^-	370, 1.002	331, 0.001	298, 0.507	–[a]	–	–
(**2**)	295, 0.369	265, 0.424	261, 0.266	345, 0.422	287, 0.339	271, 0.005
(**2**)+benzoate	230, 0.476	267, 0.352	259, 0.319	349, 0.397	291, 0.336	275, 0.063
(**2**)+F^-	299, 0.532	271, 0.915	266, 0.179	–[a]	–	–
(**3**)	332, 0.140	321, 0.457	288, 0.331	483, 0.094	363, 0.153	317, 0.501
(**3**)+benzoate	361, 0.895	346, 0.079	312, 0.208	517, 0.123	382, 0.209	343, 0.545
(**3**)+F^-	359, 1.318	320, 0.204	300, 0.265	416, 1.382	324, 0.247	317, 0.208
(**4**)	292, 0.070	272, 0.494	255, 0.121	387, 0.003	299, 0.772	286, 0.725
(**4**)+benzoate	321, 0.177	285, 0.504	275, 0.293	406, 0.186	301, 0.800	299, 0.358
(**4**)+F^-	325, 0.258	289, 1.591	266, 0.508	401, 0.230	305, 1.611	294, 0.464

[a] Excited-state geometry optimization did not converge.

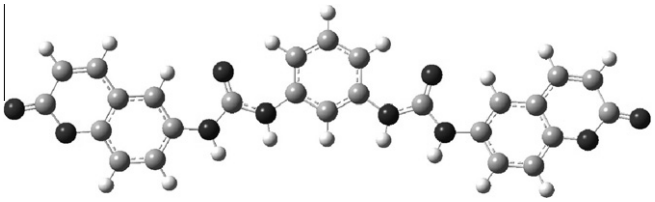

Fig. 18. DFT optimized geometry of **5**.

out for the six lowest excited states of singlet spin multiplicity. In this way information relevant to the low-energy absorption spectrum is obtained. Subsequently, geometry optimization was carried out for the first excited state, using TDDFT, resulting in information regarding the emission spectra of the systems of interest. All the calculations were carried out with the aid of Gaussian 09 suite of programs [18], and the solvent was included using the PCM model [19].

4.1. Results on the optimum geometries

The optimum geometries of the receptors are as given in Fig. 16 (with the bond lengths in Angstrom units and **a** and **b** as indicated for receptor **1**). The optimum geometries of ground and the first excited electronic states of the complexes with benzoate anion are listed in Fig. 17, where in all cases **a** and **b** are as indicated for the case of receptor **1**.

The results of the calculations show higher binding energies for complexes of receptors **1** and **3**, i.e. those containing the NO_2 moiety, and this indicates increased sensing capacity for these receptors [20]. As shown in the molecular structure of the complexes with benzoate anion, binding is through dual hydrogen bonding, resulting in elongation of the two N–H bonds of the receptors in the complexes. There are some small variations in the minimum energy geometry of the excited state, compared to the ground state minimum, such as smaller O···H distances and larger N–H distances, indicating "tighter" hydrogen bonding in the excited-state geometries.

The optimum ground-state geometries of receptors **1**–**4** with fluoride anion were also calculated (Fig. S6), and **(1)+F**$^-$ and **(2)+F**$^-$ are not planar while **(3)+F**$^-$ and **(4)+F**$^-$ are planar structures.

4.2. Excited state energies, absorption and emission spectra

In Table 3, the calculated absorption and emission maxima are listed for the four receptors and the corresponding four complexes. In all cases a red shift is found in the spectra of the complexes with respect to the spectra of the corresponding receptors. The absorption and emission spectra, as given by Gaussian 09, are listed in Fig. S7 (Supporting information), where the vertical lines correspond to the calculated levels and oscillator strengths. As shown in Table 3 and Fig. S7, for receptor **1**, the observed broad peak at 330 nm is well reproduced by the theoretical calculations while the corresponding maxima in the complexes are calculated at 361 nm for **1**.benzoate (experimental at 348 nm) and at 370 nm for **1.F**$^-$ (experimental at 455 nm). In general, the calculations are in good agreement with experiment regarding the absorption maxima of the receptors alone and less so for those of the complexes, but they are in general agreement regarding the observed

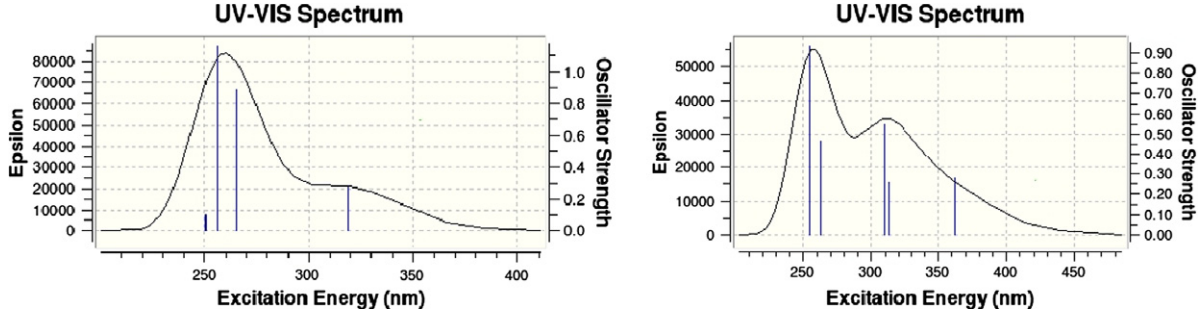

(a) Absorption (b) Emission

Fig. 19. Low-energy absorption and emission spectra of receptor **5**.

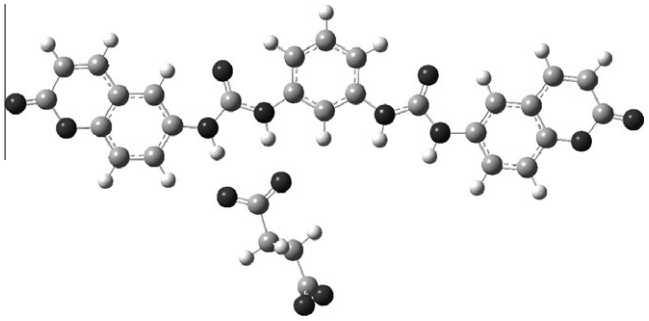

Fig. 20. Optimized geometry of the complex of **5** succinate.

red shifts. The calculated emission peaks are in variable agreement with the experimental: for receptor **1** the observed peak at 420 nm (when excited at 380 nm) is calculated at 485 nm for the receptor alone and at 504 nm for **1** + benzoate. For receptor **2** with experimental peak at 369 nm the calculated is at 345 for the receptor alone and at 349 nm for **2** + benzoate. The reduction in intensity is not predicted for **1** + benzoate while it is reproduced for **2** + benzoate (cf. Table 3). For receptor **3**, the observed fluorescence peak at 437 nm is calculated at 483 nm and 517 nm for **3** + benzoate, while for receptor **4** the observed peak at 425 nm is calculated at 387 nm and at 406 nm for **4** + benzoate. For both receptors **3** and **4** the calculated transition probability in the complexes is not reduced with respect to the receptors alone.

The excited states of the receptors with significant transition probability retain their character in the corresponding complexes, i.e. the excitations involve mainly orbitals of the receptor molecules. In Fig. S8, electron density plots are given for the lowest unoccupied orbital (LUMO) and the 4 highest occupied (HOMO, HOMO-1, HOMO-2 and HOMO-3) calculated for the complex of receptor **1** with benzoate anion, at the ground state geometry and at the geometry of the lowest excited state. These orbitals are involved in the excitations contributing to the excited states corresponding to the absorption and emission maxima. As shown, the contribution of the benzoate orbitals is minimal and mainly for the HOMO-3 orbital. Similar pictures are obtained for the other complexes as well, regarding the orbitals involved in the relevant excitations, and as a result it may be concluded that there is no significant photoinduced electron transfer involving the benzoate, although there is a degree of PET within the different parts of the receptor molecules, for example in the excitations HOMO-2 → LUMO and HOMO-3 → LUMO, for receptor **1** cf. Fig. S8.

4.3. Calculations on receptor 5

It was very difficult to converge the geometry optimization calculations on receptor **5**. Some results are presented here, obtained by DFT/B3LYP 6-31+G(dp) and TDDFT/B3LYP 6-31+G(dp) calculations. The geometry of the ground electronic state is a planar structure as shown below, with the N–H distances, from left to right in the picture of 1.01125, 1.01113, 1.01117 and 1.01129 Angstrom units (Fig. 18).

The low-energy absorption and emission spectra of receptor **5** as obtained are also displayed in Fig. 19.

Upon complexation with succinate di-anion, the only stable structure obtained involves binding only at a single COO^- moiety (Fig. 20), consistent with Mode **B** of complexation with binding energy of 0.71 eV. The relevant bond lengths are (from the left) N–H 1.03983 and 1.03954 and O···H 1.78769 and 1.77853 Angstrom units.

5. Conclusions

In conclusion, '*fluorophore–spacer–receptor*' based receptors **1**–**2** and '*fluorophore–receptor*' based receptors **3**–**4** have been designed and synthesized. The receptors are comprised of thiourea binding site and coumarin fluorophore. Receptor **1** shows strong binding to benzoate over fluoride ion by exhibiting the changes in fluorescence and color. Receptors **3** and **4**, which are '*fluorophore–receptor*' model based, are not promising compared to **1** and **2** in the sensing of anions. In this context, work to develop the practical colorimetric coumarin – based sensors for recognition of the anions especially F^- and carboxylates in aqueous solution is underway in the laboratory. However, we have also represented the use of coumarin linked urea in devising ditopic receptor **5** that are more sensible to the dicarboxylates in organic solvent. The interaction study reveals that receptor **5** is capable of distinguish isomeric aromatic dicarboxylates with moderate binding constant values. Further investigations into steric and electronic effects in similar pre-organized hosts or receptors are ongoing. The results of the theoretical calculations show differences in the geometries of the complexes, depending on the receptor and the anion and differences in the binding energies, indicating that both the presence of the nitrophenyl group in receptors **1** and **3** (but not in **2** and **4**) as well as the existence of the spacer group receptors **1** and **2** (but not in **3** and **4**) affect the efficiency of anion recognition by the different receptors.

Acknowledgment

K.G. thanks CSIR, New Delhi, India for financial support.

Appendix A. Supplementary material

Supplementary data associated with this article can be found, in the online version, at doi:10.1016/j.molstruc.2011.08.004.

Synthesis of **1** and **2**, Stern–Volmer plots of **1**, F^- induced change in emission of 2, Stern-Volmer plot of **5**, Crystal data of **2** and **4**, ^1H NMR of **3** in absence and presence of F^- and $C_6H_5COO^-$, Optimum ground-state geometries of receptors **1**–**4** with F^-, Absorption and emission spectra of **1**–**4** and their complexes with benzoate and F^-,Electron density plot for the complex **1**.$C_6H_5COO^-$.

References

[1] (a) M. Martinez, F. Sancenon, Chem. Rev. 103 (2003) 4419;
(b) A.P. De Silva, H.Q.N. Gunaratne, T. Gunnlaugsson, A.J.M. Huxley, C.P. McCoy, J.T. Rademacher, T.E. Rice, Chem. Soc. Rev. 97 (1997) 1515;
(c) C. Caltagirone, P.A. Gale, Chem. Soc. Rev. 38 (2009) 520.
[2] M.D. Lankshear, P.D. Beer, Coord. Chem. Rev. 250 (2006) 3142.
[3] P. Blondean, J. Benet-Buchholz, J. de Mendoza, New J. Chem. 31 (2007) 736. and references cited therein.
[4] C. Schmuck, U. Machon, Eur. J. Org. Chem. (2006) 4385.
[5] J.M. Linares, D. Powell, K. Bowman-James, Coord. Chem. Rev. 240 (2003) 37.
[6] K. Ghosh, S. Adhikari, Tetrahedron Lett. 47 (2006) 8165.
[7] (a) T. Gunnlaugsson, A.P. Davis, M. Glynn, Chem. Commun. (2001) 2556;
(b) J. Kang, H.S. Kim, D.O. Jang, Tetrahedron Lett. 46 (2005) 6079.
[8] P.T. Chou, G.R. Wu, C.Y. Wei, C.C. Cheng, C.P. Chang, F.T. Hung, J. Phys. Chem B. 104 (2000) 7818.
[9] S.J. Brooks, P.A. Gale, M.E. Light, Chem. Commun. (2006) 4344.
[10] (a) D. Esteban-Gomez, L. Fabbrizzi, M. Licchelli, J. Org. Chem. 70 (2005) 5717;
(b) L.S. Evans, P.A. Gale, M.E. Light, R. Quesada, New J. Chem. 30 (2006) 1019;
(c) T. Gunnlaugsson, P.E. Kruger, P. Jensen, F.M. Pfeffer, G.M. Hussey, Tetrahedron Lett. 44 (2003) 8909;
(d) S.H. Lee, H.J. Kim, Y.O. Lee, J. Vicens, J.S. Kim, Tetrahedron Lett. 47 (2006) 4373;
(e) Q. Wang, Y. Xie, Y. Ding, X. Li, W. Zhu, Chem. Commun. 46 (2010) 3669.
[11] (a) L. Fabbrizzi, M. Licchelli, E. Monzani, Org. Biomol. Chem. 3 (2005) 1495;
(b) V. Amendola, D. Esteban-Gomez, L. Fabbrizzi, M. Licchelli, Acc. Chem. Res. 39 (2006) 343;
(c) M. Bonizzoni, L. Fabbrizzi, A. Taglietti, F. Tiengo, Eur. J. Org. Chem. (2006) 3567.

[12] D.H. Lee, H.Y. Lee, K.H. Lee, J.-I. Hong, Chem. Commun. (2001) 1188.
[13] C. Roussel, M. Roman, F. Andreoli, A.D. Rio, R. Faure, N. Vanthuyne, Chirality 18 (2006) 762.
[14] (a) P. Piatek, J. Jurczak, Chem. Commun. (2002) 2450;
(b) S. Camilo, P.A. Gale, M.B. Hursthouse, M.E. Light, Org. Biomol. Chem. 1 (2003) 741.
[15] R.G. Parr, W. Yang, Annu. Rev. Phys. Chem. 46 (1995) 701.
[16] (a) M.J.G. Peach, P. Benfield, T. Helgaker, D.J.J. Tozer, Chem. Phys. 128 (2008) 044118;
(b) T. Yanai, D. Tew, N. Handy, Chem. Phys. Lett. 393 (2004) 51.
[17] M.A.L. Marques, E.K.U. Gross, Annu. Rev. Phys. Chem. 55 (2004) 427.
[18] M.J. Frisch, G.W. Trucks, H.B. Schlegel, G.E. Scuseria, M.A. Robb, J.R. Cheeseman, J.A. Montgomery, Jr., T. Vreven, K.N. Kudin, J.C. Burant, J.M. Millam, S.S. Iyengar, J. Tomasi, V. Barone, B. Mennucci, M. Cossi, G. Scalmani, N. Rega, G.A. Petersson, H. Nakatsuji, M. Hada, M. Ehara, K. Toyota, R. Fukuda, J. Hasegawa, M.T. Ishida, Nakajima, Y. Honda, O. Kitao, H. Nakai, M. Klene, X. Li, J.E. Knox, H.P. Hratchian, J.B. Cross, C. Adamo, J. Jaramillo, R. Gomperts, R.E. Stratmann, O. Yazyev, A.J. Austin, R. Cammi, C. Pomelli, J.W. Ochterski, P.Y. Ayala, K. Morokuma, G.A. Voth, P. Salvador, J.J.V.G. Dannenberg, Zakrzewski, S. Dapprich, A.D. Daniels, M.C. Strain, O. Farkas, D.K. Malick, A.D. Rabuck, K. Raghavachari, J.B. Foresman, J.V. Ortiz, Q. Cui, A.G. Baboul, S. Clifford, J. Cioslowski, B.B. Stefanov, G. Liu, A. Liashenko, P. Piskorz, I. Komaromi, R.L. Martin, D.J. Fox, T. Keith, M.A. Al-Laham, C.Y. Peng, A. Nanayakkara, M. Challacombe, P.M.W. Gill, B. Johnson, W. Chen, M.W. Wong, C. Gonzalez, J.A. Pople, Gaussian 09 (Revision A.1), Gaussian, Inc., Wallingford CT, 2004.
[19] (a) M. Cozi, G. Scalmani, N. Rega, V. Barone, J. Chem. Phys. 117 (2002) 43;
(b) A. Pedone, J. Bloino, S. Monti, G. Prampolini, V. Barone, Phys. Chem. Chem. Phys. 12 (2010) 1000.
[20] (a) K. Ghosh, G. Masanta, R. Froehlich, I.D. Petsalakis, G. Theodorakopoulos, J. Phys. Chem. B 113 (2009) 7800;
(b) I.D. Petsalakis, N. Tagmatarchis, G. Rotas, G. Theodorakopoulos, J. Mol. Struct.: THEOCHEM 807 (2007) 11.